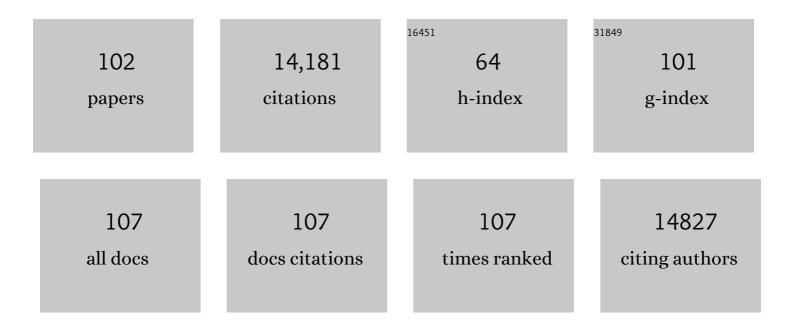
Holger Stark

List of Publications by Year in descending order

Source: https://exaly.com/author-pdf/5344383/publications.pdf Version: 2024-02-01



HOLCED STADE

#	Article	IF	CITATIONS
1	Conformational rearrangements upon start codon recognition in human 48S translation initiation complex. Nucleic Acids Research, 2022, 50, 5282-5298.	14.5	15
2	Structural insights into how Prp5 proofreads the pre-mRNA branch site. Nature, 2021, 596, 296-300.	27.8	28
3	Structural Insights into the Roles of Metazoan-Specific Splicing Factors in the Human Step 1 Spliceosome. Molecular Cell, 2020, 80, 127-139.e6.	9.7	26
4	Atomic-resolution protein structure determination by cryo-EM. Nature, 2020, 587, 157-161.	27.8	454
5	Mechanism of protein-guided folding of the active site U2/U6 RNA during spliceosome activation. Science, 2020, 370, .	12.6	50
6	Molecular architecture of the human 17S U2 snRNP. Nature, 2020, 583, 310-313.	27.8	63
7	Discovery of a Regulatory Subunit of the Yeast Fatty Acid Synthase. Cell, 2020, 180, 1130-1143.e20.	28.9	40
8	Structural and Functional Analyses of the Human PDH Complex Suggest a "Division-of-Labor― Mechanism by Local E1 and E3 Clusters. Structure, 2019, 27, 1124-1136.e4.	3.3	23
9	Protein engineering of a ubiquitin-variant inhibitor of APC/C identifies a cryptic K48 ubiquitin chain binding site. Proceedings of the National Academy of Sciences of the United States of America, 2019, 116, 17280-17289.	7.1	22
10	Structural Insights into Nuclear pre-mRNA Splicing in Higher Eukaryotes. Cold Spring Harbor Perspectives in Biology, 2019, 11, a032417.	5.5	141
11	Posing the APC/C E3 Ubiquitin Ligase to Orchestrate Cell Division. Trends in Cell Biology, 2019, 29, 117-134.	7.9	101
12	Structure and Conformational Dynamics of the Human Spliceosomal Bact Complex. Cell, 2018, 172, 454-464.e11.	28.9	175
13	Cryo-EM in drug discovery: achievements, limitations and prospects. Nature Reviews Drug Discovery, 2018, 17, 471-492.	46.4	304
14	Cryo-EM structure of a human spliceosome activated for step 2 of splicing. Nature, 2017, 542, 318-323.	27.8	207
15	Ribosome dynamics during decoding. Philosophical Transactions of the Royal Society B: Biological Sciences, 2017, 372, 20160182.	4.0	76
16	Cryo-EM Structure of a Pre-catalytic Human Spliceosome Primed for Activation. Cell, 2017, 170, 701-713.e11.	28.9	217
17	Topology and structure of an engineered human cohesin complex bound to Pds5B. Nature Communications, 2016, 7, 12523.	12.8	42
18	Mechanism of APC/C ^{CDC20} activation by mitotic phosphorylation. Proceedings of the National Academy of Sciences of the United States of America, 2016, 113, E2570-8.	7.1	112

#	Article	IF	CITATIONS
19	biGBac enables rapid gene assembly for the expression of large multisubunit protein complexes. Proceedings of the National Academy of Sciences of the United States of America, 2016, 113, E2564-9.	7.1	263
20	Cryo-EM of Mitotic Checkpoint Complex-Bound APC/C Reveals Reciprocal and Conformational Regulation of Ubiquitin Ligation. Molecular Cell, 2016, 63, 593-607.	9.7	123
21	Molecular architecture of the <i>Saccharomyces cerevisiae</i> activated spliceosome. Science, 2016, 353, 1399-1405.	12.6	165
22	The pathway to GTPase activation of elongation factor SelB on the ribosome. Nature, 2016, 540, 80-85.	27.8	93
23	Dual RING E3 Architectures Regulate Multiubiquitination and Ubiquitin Chain Elongation by APC/C. Cell, 2016, 165, 1440-1453.	28.9	126
24	Sample preparation of biological macromolecular assemblies for the determination of high-resolution structures by cryo-electron microscopy. Microscopy (Oxford, England), 2016, 65, 23-34.	1.5	43
25	Molecular architecture of the human U4/U6.U5 tri-snRNP. Science, 2016, 351, 1416-1420.	12.6	170
26	Nanobodies: site-specific labeling for super-resolution imaging, rapid epitope-mapping and native protein complex isolation. ELife, 2015, 4, e11349.	6.0	177
27	Structure of the E. coli ribosome–EF-Tu complex at <3Âà resolution by Cs-corrected cryo-EM. Nature, 2015, 520, 567-570.	27.8	338
28	ProteoPlex: stability optimization of macromolecular complexes by sparse-matrix screening of chemical space. Nature Methods, 2015, 12, 859-865.	19.0	87
29	RING E3 mechanism for ubiquitin ligation to a disordered substrate visualized for human anaphase-promoting complex. Proceedings of the National Academy of Sciences of the United States of America, 2015, 112, 5272-5279.	7.1	80
30	Molecular Basis of Transcription-Coupled Pre-mRNA Capping. Molecular Cell, 2015, 58, 1079-1089.	9.7	109
31	Expression of enterovirus 71 virus-like particles in transgenic enoki (Flammulina velutipes). Applied Microbiology and Biotechnology, 2015, 99, 6765-6774.	3.6	4
32	GraDeR: Membrane Protein Complex Preparation for Single-Particle Cryo-EM. Structure, 2015, 23, 1769-1775.	3.3	96
33	Mechanism of Polyubiquitination by Human Anaphase-Promoting Complex: RING Repurposing for Ubiquitin Chain Assembly. Molecular Cell, 2014, 56, 246-260.	9.7	98
34	Structural Basis of Assembly Chaperone- Mediated snRNP Formation. Molecular Cell, 2013, 49, 692-703.	9.7	82
35	Electron microscopy structure of human APC/CCDH1–EMI1 reveals multimodal mechanism of E3 ligase shutdown. Nature Structural and Molecular Biology, 2013, 20, 827-835.	8.2	82
36	Energy barriers and driving forces in tRNA translocation through the ribosome. Nature Structural and Molecular Biology, 2013, 20, 1390-1396.	8.2	150

#	Article	IF	CITATIONS
37	Structural Determinants and Mechanism of Mammalian CRM1 Allostery. Structure, 2013, 21, 1350-1360.	3.3	17
38	Automated correlation of single particle tilt pairs for Random Conical Tilt and Orthogonal Tilt Reconstructions. Journal of Structural Biology, 2013, 181, 149-154.	2.8	5
39	Structural basis for cooperativity of CRM1 export complex formation. Proceedings of the National Academy of Sciences of the United States of America, 2013, 110, 960-965.	7.1	64
40	Novel insights into the architecture and protein interaction network of yeast eIF3. Rna, 2012, 18, 2306-2319.	3.5	13
41	APC15 mediates CDC20 autoubiquitylation by APC/CMCC and disassembly of the mitotic checkpoint complex. Nature Structural and Molecular Biology, 2012, 19, 1116-1123.	8.2	118
42	Substrate binding on the APC/C occurs between the coactivator Cdh1 and the processivity factor Doc1. Nature Structural and Molecular Biology, 2011, 18, 6-13.	8.2	89
43	Structure of the Lassa Virus Nucleoprotein Revealed by X-ray Crystallography, Small-angle X-ray Scattering, and Electron Microscopy. Journal of Biological Chemistry, 2011, 286, 38748-38756.	3.4	47
44	Chromatin Affinity Purification and Quantitative Mass Spectrometry Defining the Interactome of Histone Modification Patterns. Molecular and Cellular Proteomics, 2011, 10, M110.005371.	3.8	74
45	An Approach for De Novo Structure Determination of Dynamic Molecular Assemblies by Electron Cryomicroscopy. Structure, 2010, 18, 667-676.	3.3	22
46	Ribosome dynamics and tRNA movement by time-resolved electron cryomicroscopy. Nature, 2010, 466, 329-333.	27.8	400
47	Characterization of purified human B ^{act} spliceosomal complexes reveals compositional and morphological changes during spliceosome activation and first step catalysis. Rna, 2010, 16, 2384-2403.	3.5	142
48	Merging Molecular Electron Microscopy and Mass Spectrometry by Carbon Film-assisted Endoproteinase Digestion. Molecular and Cellular Proteomics, 2010, 9, 1729-1741.	3.8	10
49	The MIS12 complex is a protein interaction hub for outer kinetochore assembly. Journal of Cell Biology, 2010, 190, 835-852.	5.2	196
50	GraFix: Stabilization of Fragile Macromolecular Complexes for Single Particle Cryo-EM. Methods in Enzymology, 2010, 481, 109-126.	1.0	187
51	3D Cryo-EM Structure of an Active Step I Spliceosome and Localization of Its Catalytic Core. Molecular Cell, 2010, 40, 927-938.	9.7	43
52	Characterization of Tailor-Made Copolymers of Oligo(ethylene glycol) Methyl Ether Methacrylate and <i>N</i> , <i>N</i> -Dimethylaminoethyl Methacrylate as Nonviral Gene Transfer Agents: Influence of Macromolecular Structure on Gene Vector Particle Properties and Transfection Efficiency. Biomacromolecules, 2010, 11, 39-50.	5.4	61
53	Systematic Analysis of Human Protein Complexes Identifies Chromosome Segregation Proteins. Science, 2010, 328, 593-599.	12.6	465
54	Cryonegative Staining of Macromolecular Assemblies. Methods in Enzymology, 2010, 481, 127-145.	1.0	17

#	Article	IF	CITATIONS
55	DNA translocation activity of the multifunctional replication protein ORF904 from the archaeal plasmid pRN1. Nucleic Acids Research, 2009, 37, 6831-6848.	14.5	9
56	Structural mapping of spliceosomes by electron microscopy. Current Opinion in Structural Biology, 2009, 19, 96-102.	5.7	38
57	Parallel, distributed and GPU computing technologies in single-particle electron microscopy. Acta Crystallographica Section D: Biological Crystallography, 2009, 65, 659-671.	2.5	24
58	Exon, intron and splice site locations in the spliceosomal B complex. EMBO Journal, 2009, 28, 2283-2292.	7.8	46
59	Snapshots of the RNA editing machine in trypanosomes captured at different assembly stages in vivo. EMBO Journal, 2009, 28, 766-778.	7.8	64
60	Self-assembly of a nanoscale DNA box with a controllable lid. Nature, 2009, 459, 73-76.	27.8	1,464
61	Reconstitution of both steps of Saccharomyces cerevisiae splicing with purified spliceosomal components. Nature Structural and Molecular Biology, 2009, 16, 1237-1243.	8.2	150
62	Self-Assembly of Ternary Insulinâ^'Polyethylenimine (PEI)â^'DNA Nanoparticles for Enhanced Gene Delivery and Expression in Alveolar Epithelial Cells. Biomacromolecules, 2009, 10, 2912-2920.	5.4	42
63	The Evolutionarily Conserved Core Design of the Catalytic Activation Step of the Yeast Spliceosome. Molecular Cell, 2009, 36, 593-608.	9.7	255
64	Structure of the Anaphase-Promoting Complex/Cyclosome Interacting with a Mitotic Checkpoint Complex. Science, 2009, 323, 1477-1481.	12.6	195
65	Localization of Prp8, Brr2, Snu114 and U4/U6 proteins in the yeast tri-snRNP by electron microscopy. Nature Structural and Molecular Biology, 2008, 15, 1206-1212.	8.2	68
66	GraFix: sample preparation for single-particle electron cryomicroscopy. Nature Methods, 2008, 5, 53-55.	19.0	476
67	An Assembly Chaperone Collaborates with the SMN Complex to Generate Spliceosomal SnRNPs. Cell, 2008, 135, 497-509.	28.9	189
68	Structure of yeast U6 snRNPs: Arrangement of Prp24p and the LSm complex as revealed by electron microscopy. Rna, 2008, 14, 2528-2537.	3.5	25
69	Towards understanding selenocysteine incorporation into bacterial proteins. Biological Chemistry, 2007, 388, 1061-1067.	2.5	16
70	Composition and three-dimensional EM structure of double affinity-purified, human prespliceosomal A complexes. EMBO Journal, 2007, 26, 1737-1748.	7.8	178
71	Spontaneous reverse movement of mRNA-bound tRNA through the ribosome. Nature Structural and Molecular Biology, 2007, 14, 318-324.	8.2	87
72	Structural insight into filament formation by mammalian septins. Nature, 2007, 449, 311-315.	27.8	406

#	Article	IF	CITATIONS
73	Protein Composition and Electron Microscopy Structure of Affinity-Purified Human Spliceosomal B Complexes Isolated under Physiological Conditions. Molecular and Cellular Biology, 2006, 26, 5528-5543.	2.3	265
74	Organization of Core Spliceosomal Components U5 snRNA Loop I and U4/U6 Di-snRNP within U4/U6.U5 Tri-snRNP as Revealed by Electron Cryomicroscopy. Molecular Cell, 2006, 24, 267-278.	9.7	70
75	CRYO-ELECTRON MICROSCOPY OF SPLICEOSOMAL COMPONENTS. Annual Review of Biophysics and Biomolecular Structure, 2006, 35, 435-457.	18.3	82
76	Crystal structure of a core spliceosomal protein interface. Proceedings of the National Academy of Sciences of the United States of America, 2006, 103, 1266-1271.	7.1	70
77	Structure of the Hepatitis C Virus IRES Bound to the Human 80S Ribosome: Remodeling of the HCV IRES. Structure, 2005, 13, 1695-1706.	3.3	163
78	Architecture of the Human Ndc80-Hec1 Complex, a Critical Constituent of the Outer Kinetochore. Journal of Biological Chemistry, 2005, 280, 29088-29095.	3.4	157
79	Aerosolized nanogram quantities of plasmid DNA mediate highly efficient gene delivery to mouse airway epithelium. Molecular Therapy, 2005, 12, 493-501.	8.2	64
80	Major Conformational Change in the Complex SF3b upon Integration into the Spliceosomal U11/U12 di-snRNP as Revealed by Electron Cryomicroscopy. Molecular Cell, 2005, 17, 869-883.	9.7	70
81	Localization of the Coactivator Cdh1 and the Cullin Subunit Apc2 in a Cryo-Electron Microscopy Model of Vertebrate APC/C. Molecular Cell, 2005, 20, 867-879.	9.7	85
82	Advantages of CCD detectors for de novo three-dimensional structure determination in single-particle electron microscopy. Journal of Structural Biology, 2005, 151, 92-105.	2.8	59
83	Structural Basis for the Function of the Ribosomal L7/12 Stalk in Factor Binding and GTPase Activation. Cell, 2005, 121, 991-1004.	28.9	354
84	Three-dimensional structure of a pre-catalytic human spliceosomal complex B. Nature Structural and Molecular Biology, 2004, 11, 463-468.	8.2	66
85	The Three-dimensional Structure of an Ionotropic Glutamate Receptor Reveals a Dimer-of-dimers Assembly. Journal of Molecular Biology, 2004, 344, 435-442.	4.2	113
86	Quaternary Structure of the European Spiny Lobster (Palinurus elephas) 1×6-mer Hemocyanin from cryoEM and Amino Acid Sequence Data. Journal of Molecular Biology, 2003, 325, 99-109.	4.2	24
87	Molecular Architecture of the Multiprotein Splicing Factor SF3b. Science, 2003, 300, 980-984.	12.6	246
88	Experience with liquid helium cooling in electron cryomicroscopy. Microscopy and Microanalysis, 2003, 9, 397-397.	0.4	0
89	Three-Dimensional Electron Cryomicroscopy of Ribosomes. Current Protein and Peptide Science, 2002, 3, 79-91.	1.4	22
90	Three-Dimensional Structure of the Anaphase-Promoting Complex. Molecular Cell, 2001, 7, 907-913.	9.7	69

#	Article	IF	CITATIONS
91	Efficient encapsulation of antisense oligonucleotides in lipid vesicles using ionizable aminolipids: formation of novel small multilamellar vesicle structures. Biochimica Et Biophysica Acta - Biomembranes, 2001, 1510, 152-166.	2.6	344
92	Arrangement of RNA and proteins in the spliceosomal U1 small nuclear ribonucleoprotein particle. Nature, 2001, 409, 539-542.	27.8	210
93	Single-particle electron cryo-microscopy: towards atomic resolution. Quarterly Reviews of Biophysics, 2000, 33, 307-369.	5.7	535
94	Structure of a molluscan hemocyanin didecamer (HtH1 from Haliotis tuberculata) at 12 Ã resolution by cryoelectron microscopy. Journal of Molecular Biology, 2000, 298, 21-34.	4.2	55
95	Elucidating the medium-resolution structure of ribosomal particles: an interplay between electron cryo-microscopy and X-ray crystallography. Structure, 1999, 7, 931-941.	3.3	41
96	Structure of influenza haemagglutinin at neutral and at fusogenic pH by electron cryo-microscopy. FEBS Letters, 1999, 463, 255-259.	2.8	90
97	Correlation of the expansion segments in mammalian rRNA with the fine structure of the 80 s ribosome; a cryoelectron microscopic reconstruction of the rabbit reticulocyte ribosome at 21 å resolution. Journal of Molecular Biology, 1998, 279, 403-421.	4.2	62
98	A new model for the three-dimensional folding of Escherichia coli 16 s ribosomal RNA. III †. The topography of the functional centre 1 â€Paper II in this series is an accompanying paper, Mueller & Brimacombe (1997b). 1Edited by D. E. Draper. Journal of Molecular Biology, 1997, 271, 566-587.	4.2	76
99	Visualization of elongation factor Tu on the Escherichia coli ribosome. Nature, 1997, 389, 403-406.	27.8	342
100	Stacked bilayer helices: a new structural organization of amphiphilic molecules. Ultramicroscopy, 1996, 62, 133-139.	1.9	43
101	Electron radiation damage to protein crystals of bacteriorhodopsin at different temperatures. Ultramicroscopy, 1996, 63, 75-79.	1.9	81
102	The 70S Escherichia coli ribosome at 23 å resolution: fitting the ribosomal RNA. Structure, 1995, 3, 815-821.	3.3	237